Optical water type discrimination and tuning remote sensing band-ratio algorithms: application to retrieval of chlorophyll and $K_d(490)$ in the Irish and Celtic Seas.

David McKee[1], Alex Cunningham and Agnes Dudek

Scottish Universities Physics Alliance, Physics Department, University of Strathclyde, 107 Rottenrow, Glasgow, G4 ONG, Scotland.

[1]corresponding author,

email: david.mckee@strath.ac.uk

tel: +44 (0)141 548 3474

fax: +44 (0)141 552 2891

Keywords: ocean colour, shelf seas, chlorophyll, diffuse attenuation, UK, Irish Sea.

Abstract

This paper assesses the feasibility of applying remote sensing algorithms based on blue/green reflectance ratios to Case 2 waters. Two algorithms from the SeaDAS (NASA) image processing package, *OC4v4* for surface chlorophyll concentration, *Chl*, and *K(490)* for the attenuation coefficient for downward irradiance at 490 nm, K_d(490), were investigated using an extensive set of observations from the Irish and Celtic Seas. *In situ* data from a profiling radiometer were used as inputs for the algorithms to avoid uncertainties in atmospheric correction procedures, and direct measurements of *Chl* and K_d490 and were used for validation purposes. The standard versions of the algorithms performed poorly: *OC4v4* generally overestimated *Chl* (with a very low coefficient of determination), and *K(490)* progressively underestimated K_d490 for values greater than 0.3 m^{-1}. A two-step procedure for level 2 product generation was therefore devised in which the numerical coefficients of *OC4v4* and *K*(*490*) were tuned for the two optical water types known to occur most frequently in this region (McKee and Cunningham 2006) by statistical regression on a data set of 102 stations from the Irish and Celtic Seas. The water types were distinguished by the magnitude of their normalised water leaving radiance signals at 665 nm, *nLw*(*665*), and appropriate versions of the tuned algorithms applied to each water type. When this procedure was tested on an independent data set of 19 stations from the Bristol Channel, *Chl* values were recovered with an RMS error of 0.36 mg m^{-3} and $K_d(490)$ values with an RMS error of 0.095 m^{-1}. The identification of water types from water-leaving radiance signals, and the application of band-ratio algorithms tuned for specific water types, may therefore provide a simple means of improving the quality of remote sensing products in optically complex shelf seas.

1. Introduction

There are strong practical reasons for using satellite remote sensing to study the extensive shelf seas of Northern Europe. The Irish, North and Baltic Seas are all influenced by the adjacent land masses and suffer from eutrophication, harmful algal blooms and the re-suspension of contaminated sediments. These seas are more optically complex than oceanic waters, and are largely classified as Case 2 in the scheme proposed by Morel and Prieur (1977). The development of effective ocean colour algorithms for Case 2 waters poses a continuing challenge (Sathyendranath 2000), and several studies have demonstrated that a widely used class of algorithms based on blue-green reflectance ratios perform poorly in coastal regions (Gohin et al 2002, Wang and Cota 2003). However these algorithms are still commonly used to generate standard remote sensing products that are widely distributed to the user community. Their continued popularity stems from the fact that they are computationally undemanding and have been empirically validated against a large-scale oceanographic data set. The object of this paper is to assess the feasibility of improving the quality of remote sensing products generated by simple band-ratio algorithms in optically complex shelf seas. The approach adopted is to tune the numerical coefficients of the algorithms for identifiable water types rather than geographic locations. This allows for the possibility that the spatial occurrence of specific water types may vary seasonally or in response to physical forcing factors. The effective targeting of such algorithms requires the fulfilment of two conditions. First, water types with distinct optical characteristics should occur in the region. Secondly, these water types should be identifiable from their reflectance signatures. A recent study of the Irish and Celtic Seas demonstrated that these waters frequently fall into two optical classes distinguished by different relationships between their inherent

optical properties (McKee and Cunningham 2006). Consequently these seas, which have previously been identified as a challenging region for optical remote sensing (Joint and Groom 2000, Darecki et al. 2003), appear to be a suitable testing ground for exploring the tuning and targeting of band-ratio algorithms.

Two blue-green reflectance ratio algorithms are investigated: (a) *OC4v4* (O'Reilly et al 2000) which estimates chlorophyll concentration, and (b) *K(490)* (Mueller 2000) which estimates the diffuse attenuation coefficient for downwards irradiance at 490 nm, $K_d(490)$. Both of these algorithms were designed to operate on global scales, and are therefore optimised for data sets that are dominated by clear oceanic waters. It should be noted that other types of algorithms, such as the semi-analytic GSM01 algorithm, are also tuned for global applications in this manner (Maritorena et al 2002). The presence of significant concentrations of non-algal materials in coastal waters has the potential to cause relationships between radiometry, optical properties and constituents to diverge from those that these algorithms were founded upon. In this paper we examine the performance of *OC4v4* and *K(490)* in coastal waters that have previously been found to have two distinct Case 2 optical water types (McKee and Cunningham 2006).

2. Methods

The main set of data was collected from 102 stations in the Irish and Celtic Seas at the positions shown in Figure 1 during 5 cruises in May, August and November 2001 and April and July 2002. The open waters in the south west of this region are generally low in turbidity, but significant concentrations of suspended

inorganic sediment may occur in the north east and in the major estuaries (Bowers et al. 2002, Smith et al. 2003). Levels of coloured dissolved organic matter (*CDOM*) are raised locally by river inputs, and blooms of phytoplankton may occur during spring and summer (Gowen et al. 2000, Raine et al. 2001, Smyth et al. 2002). The main data set was used to assess the performance of standard *SeaDAS* chlorophyll (*OC4v4*) and $K_d(490)$ algorithms and subsequently to adjust the numerical values of their coefficients.

An independent data set, used to assess the performance of the tuned algorithms, was collected at 19 stations in the Bristol Channel in April 2005. The Bristol Channel is strongly tidal and a wide range of turbidity levels were sampled over a short geographical range. These stations are identified separately in Figure 1.

2.1. Optical measurements

Profiles of downward irradiance (E_d) and upward radiance (L_u), were measured using a Satlantic free-fall radiometer (SPMR – SeaWiFS Profiling Multichannel Radiometer) equipped with six SeaWiFS compatible detection wavebands centred on 412, 443, 490, 510, 554 and 665 nm, and a seventh channel centred on 700 nm. The SPMR was deployed at a distance of at least 20 m from the ship to avoid shadowing, and a reference sensor (SMSR – Satlantic Multichannel Surface Reference) measured downward irradiance above the surface in the same seven wavebands. Only profiles obtained during periods of constant surface irradiance were retained for further analysis. The manufacturer's sensor calibration files were employed, and a 100 W standard lamp (Bentham CL2 calibrated to National Physical Laboratory standard) was used before and after every cruise to check that the instrument response remained within specification. Signals from the SPMR were

processed using software routines supplied by Satlantic to derive the normalized water-leaving radiance, $nL_w(\lambda)$, above surface remote sensing reflectance, $R_{rs}(\lambda)$, and the diffuse attenuation coefficient, $K_d(\lambda)$ for each channel. Total backscattering, $b_b(\lambda)$, was measured at 470 nm and 676 nm using a Hydroscat-2 (HOBI Labs). Backscattering signals were corrected for path length attenuation effects using the manufacturer's sigma correction procedure. The sigma correction parameter was calculated with a 3-term polynomial expansion (coefficients for the polynomial supplied by the manufacturer) on K_{bb}, which in turn was given by $K_{bb} = a + 0.75\ b$ (see McKee and Cunningham 2005 for further details). Particulate backscattering, $b_{bp}(\lambda)$, was obtained by subtracting values for pure water backscattering derived from the measurements of Smith and Baker (1981). A 25 cm pathlength WetLabs AC-9 was used to measure the absorption coefficient, $a_n(\lambda)$, and beam attenuation coefficient, $c_n(\lambda)$, of materials other than water at nine wavelengths (412, 440, 488, 510, 532, 555, 630, 676, 715 nm - 10 nm FWHM) across the visible spectrum. Optical blanks for the AC-9 were regularly measured using ultrapure Millipore water treated with ultraviolet light, and calibration of the two optical channels remained within the manufacturer's specifications of ±0.005 m^{-1}. Absorption and attenuation signals at 715 nm were corrected for temperature dependent water absorption (Pegau et al. 1997). Absorption signals were corrected for incomplete collection of scattered light using the Zaneveld method (Zaneveld et al. 1994). The particulate scattering coefficient (b_p) was obtained by subtraction of absorption from attenuation (c_n-a_n).

2.2. Water sample analysis

Chlorophyll samples were filtered through 25mm GF/F filters and immediately frozen (-20 °C). Once in the laboratory, the filter papers were soaked for

24 hours in neutralised 90% acetone and the absorbance of the extract measured in a custom-built spectrophotometer using 1 cm pathlength cuvettes before and after acidification with dilute hydrochloric acid. The trichromatic equations of Jeffrey and Humphrey (1975) were used to convert absorbance spectra to concentrations of chlorophyll *a* (*Chl*). All samples were measured in triplicate. Total suspended solids (*TSS*) samples were obtained by filtering 5 litres of seawater through pre-weighed 90 mm GF/F filters and rinsing with 50 ml of distilled water. Samples were stored frozen until returned to the laboratory where they were dried in an oven at 100 °C for three hours and reweighed. The concentration of mineral suspended solids (*MSS*) was obtained by re-weighing samples after they had been placed in a furnace at 500 °C for three hours, at which point it was assumed that all organic materials had been combusted. Coloured dissolved organic materials (*CDOM*) samples were filtered through 0.2 μm membrane filters, with the filtrate being collected in clean glass bottles (rinsed with acid then ultra-pure water and allowed to dry) with nalgene caps and stored under refrigeration. Absorption by *CDOM* was measured in the same custom-built spectrophotometer using 10 cm cuvettes and UV treated ultra-pure water as a reference. Since non-algal materials including mineral particles and *CDOM* were present in significant quantities at all stations, the data set fell entirely within the Case 2 classification of Morel and Prieur (1977).

2.3. Band-ratio algorithms

For the purposes of this paper, two algorithms were selected which could be expressed in simple algebraic form and applied to sea-surface normalised water leaving radiance (nL_w) and remote sensing reflectance (R_{rs}) spectra derived from SPMR measurements. These were the *OC4v4* algorithm for near-surface

chlorophyll *a* concentration (*Chl*) and the *K(490)* algorithm for the diffuse attenuation coefficient for downward planar irradiance at 490 nm, $K_d(490)$ (O'Reilly et al 2000, Mueller 2000). Both algorithms are used in the NASA *SeaDAS* image processing software package. They employ simple numerical expressions based on ratios of R_{rs} or nL_w signals in blue and green SeaWiFs wavebands. The performance of these algorithms for the Irish / Celtic Seas was tested independently of the atmospheric correction procedure by applying them to R_{rs} and nL_w derived from in situ radiometric measurements and comparing retrieved *Chl* and $K_d(490)$ values with direct measurements. *OC4v4* calculates the logarithm of the ratio of remote sensing reflectance at two wavelengths using

$$R = \log_{10}\left(\frac{R_{rs}(\lambda_1)}{R_{rs}(\lambda_2)}\right) \qquad (1)$$

where λ_1 = 443 nm, 490 nm or 510 nm (whichever gives the greatest *R*), λ_2 = 555 nm, and then estimates chlorophyll concentrations from

$$Chl = 10^{(0.366 - 3.067R + 1.930R^2 + 0.649R^3 - 1.532R^4)} \qquad (2)$$

while $K_d(490)$ is estimated from

$$K_d(490) = 0.016 + 0.15645\left[\frac{nL_w(490)}{nL_w(555)}\right]^{-1.5401} \qquad (3)$$

The numerical values of the coefficients in equations (2) and (3) were empirically determined to provide optimal performance for global applications using data sets that were more representative of the open ocean than of coastal and shelf seas (e.g. Maritorena et al 2002).

3. Results

3.1. Performance of standard algorithms

Values of $K_d(490)$ retrieved using Equation 3 are plotted against measurements from the test data set in Figure 2. The points lay close to the 1:1 line for measured values below 0.3 m^{-1}, but there was increasing divergence above this value with retrieved $K_d(490)$ values being too low by a factor of ~8. This result was in accordance with that reported by Mueller (2000). *Chl* values retrieved using *OC4v4* (Equation 2) were plotted against measured values in Figure 3. This figure showed that *OC4v4* performed poorly for this region ($r^2 = 0.16$) and had a strong tendency to overestimate chlorophyll concentrations. The mean percentage error for this data set was 140%, but estimates for individual stations were up to a factor of 6 too high. Only 18% of the *OC4v4* data points lay within the target ±35% error range specified for the SeaWiFS project (Mueller and Austin 1995). These results were consistent with those found by Froidefond et al (2002) for turbid waters in a coastal area of the Bay of Biscay. The standard forms of the *K(490)* and *OC4v4* algorithms therefore produced unsatisfactory results in the Irish and Celtic Seas

3.2. Identification of optical water types from IOPs

Figure 4 shows a plot of particulate backscattering (b_{bp}) against non-water absorption (a_n) at 676 nm for the Irish and Celtic Sea data set. The data fell into two clusters and were partitioned into two subsets with Group *A* having $b_{bp}/a_n > 0.5$ and Group *B* with $b_{bp}/a_n < 0.5$. Similar clustering was previously observed for other combinations of IOPs, including the ratio of blue to red absorption and the ratio of scattering to absorption at 676 nm. Group *A* stations had generally higher values of the backscattering ratio than Group *B*. Particulate IOPs were dominated by *MSS* for

Group *A* waters and *Chl* for Group *B* waters, indicating that optical water types could be related to differences in the composition of particulate seawater constituents. Absorption by *CDOM* at 440nm was found to vary between 0.05 and 0.25 m^{-1} and distributions were similar for both water types (McKee and Cunningham 2006).

3.3. Discrimination of water types by normalised water leaving radiance

Figure 5 shows normalised water leaving radiance spectra for 12 stations, 6 for each water type, selected for having the lowest (Group B) or highest (Group A) $nL_w(665)$ values. For approximately 90% of Group *B*, values of $nL_w(665)$ were less than 0.1 μW cm^{-2} nm^{-1} sr^{-1}, while almost 95% of Group *A* data lay above this threshold value. Similar bimodal distributions of nL_w were observed at 554 nm and 700 nm where the threshold values were 1 and 0.075 μW cm^{-2} nm^{-1} sr^{-1} respectively. Consequently, Group *A* data could be largely distinguished from Group *B* data by higher values of normalised water leaving radiances in the green and red wavebands. Distributions of nL_w overlapped to a greater extent in the blue wavelengths, where absorption by *CDOM* and minerals opposed the effect of particulate backscattering on reflectance signals. For these waters, the threshold value of $nLw(665)$ = 0.1 μW cm^{-2} nm^{-1} sr^{-1} can be used as a flag to separate data by optical water type.

3.4. Tuning algorithm coefficients for water types

Figure 6 shows measured values of $K_d(490)$ plotted against the ratio of normalised water leaving radiances at 490 and 555 nm, with the Irish / Celtic Sea data segregated by optical water type. Group A data (b_{bp}/a_n > 0.5 at 676 nm) tended to have higher values of $K_d(490)$ for a given ratio of $nL_w(490)$ / $nL_w(555)$ than corresponding Group B data. The standard *SeaDAS K(490)* algorithm, plotted as a

solid line in Figure 6, passed through the Group B data reasonably well (r^2 = 0.42), but provided a very poor fit for Group A. To overcome this problem a dual algorithm approach was developed in which the standard *K(490)* algorithm was used for Group *B* water, but a re-parameterised version of the standard algorithm was developed for Group *A* stations. The re-parameterised algorithm had the same mathematical form as the standard algorithm defined in Mueller (2000):

$$K_d(490) = 0.016 + a\left(\frac{nL_w(490)}{nL_w(555)}\right)^b \qquad (4)$$

where 0.016 m^{-1} is the diffuse attenuation coefficient for pure water at 490 nm. The coefficients *a* and *b* were determined for Group *A* data using the Marquardt-Levenburg algorithm to minimise the sum of the squared differences between observed and predicted values, and best-fit values of *a* = 0.3189 and *b* = -3.0054 were obtained. The tuned *K(490)* algorithm, plotted as a dashed line in Figure 6, gave a good fit to the Group A cluster (r^2 = 0.85) and came close to converging with the standard algorithm for high values of $nL_w(490) / nL_w(555)$. This dual algorithm for retrieving $K_d(490)$ in the Irish / Celtic Sea will be referred to as *IS-*$K_d(490)$, with subscripts *A* and *B* indicating the water-type variant:

$$\begin{aligned} IS_A - K_d(490) &= 0.016 + 0.3189x^{-3.0054} \\ IS_B - K_d(490) &= 0.016 + 0.1564x^{-1.5401} \end{aligned} \qquad (5)$$

where *x* is the ratio $nL_w(490) / nL_w(555)$, and IS_B-$K_d(490)$ is the standard *SeaDAS* algorithm .

Figure 7 shows measured *Chl* plotted against the logarithm of the maximum blue-green reflectance ratio, *R* (see Equation 1), for both optical water types found in the Irish / Celtic Sea data set. Once again the data formed clusters according to optical water type, but in this case the standard *SeaDAS* algorithm (*OC4v4*, dotted line)

provided a poor fit for both clusters. A dual-algorithm was developed incorporating two tuned algorithms, one for each water type. The algebraic form of the *OC4v4* algorithm was retained and new coefficients determined using the Marquandt-Levenburg regression algorithm. The resulting Irish / Celtic Sea regional chlorophyll algorithm can be summarised as:

$$\begin{aligned} IS_A - Chl &= 10^{\left(-0.2223 - 3.4118\,R - 3.6683\,R^2 - 2.6599\,R^3 - 0.8431\,R^4\right)} \\ IS_B - Chl &= 10^{\left(0.1948 - 2.4851\,R - 2.4062\,R^2 - 2.7332\,R^3 - 1.5733\,R^4\right)} \end{aligned} \qquad (6)$$

where R is given by Equation 1 and the subscripts A and B refer to the optical water type. Both expressions in Equation 6 resulted in $r^2 > 0.6$ for their respective data sets.

3.5 Descriptive effectiveness of the tuned algorithms

Data from the Irish and Celtic Seas were segregated into High and Low reflectance water types using the $nL_w(665)$ flag and the dual algorithms (Equations 5 and 6) were applied to the resulting grouping. Figure 8 demonstrates significantly improved recovery of $K_d(490)$ for this data set compared to the standard algorithm (Figure 2). *IS-*$K_d(490)$ values were well correlated with measured values across the entire range (r^2 = 0.91) and the regression line had a low offset (~0.04 m^{-1}) and a gradient close to unity (0.89 ± 0.06, 95% confidence). The bifurcation observed in Figure 2 was effectively eliminated. Recovery of *Chl* using the *IS-Chl* dual algorithm (Figure 9) was also significantly improved, with approximately 75% of *IS-Chl* values falling within the SeaWiFS mission target of ±35% (the RMS percentage error was 34%), and with a corresponding RMS error of 0.36 mg m^{-3}. Both of the tuned algorithms improved on the standard versions by eliminating systematic errors in retrieved parameters.

3.6. Validation of tuned algorithms

A second, independent data set collected in the Bristol Channel in April 2005 was used to perform a preliminary test of the predictive power of the dual algorithms developed above. The $nL_w(665)$ threshold value of 0.1 μW cm^{-2} nm^{-1} sr^{-1} was again used to segregate data into Groups A and B. Figure 10 shows values of $K_d(490)$ calculated using both the standard algorithm and Equation 5, plotted against in situ measurements. As before, the standard algorithm systematically underestimated $K_d(490)$ by a factor of ~8 in turbid waters, while the dual algorithm provided calculated values of $K_d(490)$ that matched in situ values across the range of measurements ($r^2 = 0.97$), with a RMS error of 0.095 m^{-1}. The retrieval of *Chl* from the dual algorithm (Equation 6) was also significantly better for the Bristol Channel data set than that provided by the standard *OC4v4* algorithm (Figure 11). Here the standard *OC4v4* algorithm systematically overestimated *Chl* by up to an order of magnitude with errors averaging 380%. There was still a small overestimate of *Chl* using the *IS-Chl* algorithm for low concentrations in highly turbid waters, but the majority of *IS-Chl* data points fell within the ±35% target, and the RMS error was 0.36 mg m^{-3}. These results are particularly encouraging because they were obtained for a reasonably broad range of turbid coastal stations outside the original sampling area.

4. Discussion

The standard *OC4v4* and *K(490)* algorithms attempt to recover qualitatively different level 2 products from remote sensing reflectance signals. *OC4v4* estimates the concentration of an optically important seawater constituent (chlorophyll) while *K(490)* estimates the value of an apparent optical property (the attenuation coefficient

for downward planar irradiance at 490 nm). The algorithms differ in the manner of their failure in the Irish and Celtic Seas, since the errors generated by *K*(*490*) are essentially systematic and progressive (Figure 2), while those of *OC4v4* have a wide spread with an overall positive bias (Figure 3). Both algorithms are essentially empirical in nature, and they incorporate coefficients whose values were derived by statistical regression from a data set dominated by oceanic waters. It is not surprising, therefore, that these algorithms perform poorly in shelf seas. What is surprising is the fact that these relatively simple algorithms can be adapted to both Group A and Group B water types, which are optically much more complex than oceanic waters, by a simple change in the values of their coefficients. The optical properties of Group B waters are largely determined by *Chl* and *CDOM*, while those of Group A waters are dominated by *MSS* and *CDOM* (McKee and Cunningham 2006). This has the effect of greatly increasing the scattering and backscattering coefficients relative to absorption in Group A waters (Figure 4), and has different implications for the two algorithms in question.

4.1 K(490)

The standard algorithm (Equation 3) assumes a monotonic, single-value relationship between $K_d(490)$ and the ratio $nL_w(490)/nL_w(555)$. Figure 5 shows that this ratio is a well-behaved function of $K_d(490)$ in both Group A and Group B stations (though the range of values for Group B stations is rather limited), but that it is no longer single valued. The fact that the higher scattering levels produced by *MSS* in Group A stations does not destroy the systematic relationship between $nL_w(490)/nL_w(555)$ and $K_d(490)$ explains why the algebraic form of the *K(490)* algorithm can be applied to this water type. On the other hand, the progressive

bifurcation of the data as the measured $K_d(490)$ value increases demonstrates that tuning of the coefficients according to water type is required.

4.2 OC4v4

OC4v4 (Equations 1 and 2) is based on the assumption that changes in the blue-green reflectance ratio are driven by the spectral characteristics of phytoplankton absorption and backscattering. The addition of either *CDOM* or *MSS* invalidates the assumed relationship between the blue-green reflectance ratio and *Chl*, since all three constituents absorb more strongly in blue than green wavelengths, while only *Chl* and *MSS* contribute to backscattering. Figure 7 shows that the result is a reduction in the value of the R_{rs} ratio used in *OC4v4*, relative to oceanic waters, for a given *Chl* value. This reduction is more marked for Group A than Group B stations, reflecting the effect of *MSS* on backscattering, and it is therefore necessary to use different coefficients for the two water types. The degree of scatter in the data plotted in Figure 7 is reflected in the relatively low coefficient of determination for the *Chl* values recovered by *IS-Chl* (Figure 9). In this case, the main advantage of the dual-algorithm approach is the reduction in the consistent tendency of *OC4v4* to over-estimate *Chl* in turbid waters rather than in the precision of recovery.

4.3 Implications.

Algorithms based on blue/green nL_w ratios often perform poorly in shelf seas and turbid coastal waters (Toole and Siegel 2001, Gohin et al 2002, Feng et al 2005). The results presented here indicate that this is not a fundamental product of algorithm structure, but rather results from variability in the inter-relationship between IOPs in different water types. The identification of optical water types using IOP groupings,

and the targeted tuning of algorithm coefficient to water type, is clearly useful for understanding relationships between remote sensing signals and concentrations of optically significant constituents in the Irish and Celtic Seas. A similar method may be useful for devising tuned algorithms for other areas of interest. Gohin et al (2005), for example, presented data from the Bay of Biscay (their Figure 4) that suggests the presence of two distinct water types. Identifying optical water types from space is a new concept that deserves further exploration. We have shown that turbid (Group A) waters can be identified using a red-wavelength nL_w flag but further work is required to facilitate e.g. discrimination of Group B from Case 1 waters. It is possible, for example, that Case 1 waters with very low *CDOM* levels would have higher reflectances in the deep blue (e.g. 412 nm) than our Group B stations. Unfortunately our regional data set does not feature Case 1 stations to test this hypothesis and a robust and complete set of flags for identifying optical water types from space remains a future target. A practical difficulty may arise from the fact that the performance of atmospheric correction algorithms over shelf seas is often degraded due to the presence of industrial aerosols and suspended minerals (Land and Haigh 1997, Moore et al. 1999, Hu et al 2000, Forget et al. 2001, Lavender et al. 2005). The degree to which this interferes with the process of identifying optical water types from space clearly requires further study.

Acknowledgements

This research was funded by the UK Natural Environment Research Council. The Remote Sensing and Data Analysis Service at Plymouth Marine Laboratory, and Dr S. J. Lavender (University of Plymouth) provided a great deal of encouragement and advice.

References

Bowers, D.G., Gaffney, S., White, M., Bowyer, P., 2002. Turbidity in the southern Irish Sea. Continental Shelf Research 22, 2115 – 2126.

Darecki, M., Weeks, A., Sagan, S., Kowalczuk, P., Kacmarek, S., 2003. Optical characteristics of two contrasting Case 2 waters and their influence on remote sensing algorithms. Continental Shelf Research 23, 237 – 250.

Feng, H., Campbell, J.W., Dowell, M.D., Moore, T.S., 2005. Modeling spectral reflectance of optically complex waters using bio-optical measurements from Tokyo Bay. Remote Sensing of Environment 99, 232 - 243.

Forget, P., Broche, P., Nandin, J.J., 2001. Reflectance sensitivity to solid suspended sediment stratification in coastal water and inversion: a case study. Remote Sensing of Environment 77, 92 – 103.

Froidefond, J.-M., Lavender, S., Laborde, P., Herbland, A., Lafon, V., 2002. SeaWiFS data interpretation in a coastal area in the Bay of Biscay. International Journal of Remote Sensing 23(5), 881 – 904.

Gohin, F., Druon, J.N., Lampert, L., 2002. A five-channel chlorophyll concentration algorithm applied to SeaWiFS data processed by *SeaDAS* in coastal waters. International Journal of Remote Sensing 23, 1639 – 1661.

Gohin, F., Loyer, S., Lunven, M., Labry, C., Froidefond, J.-M., Delmas, D., Huret, M., Herbland, A., 2005. Satellite-derived parameters for biological modelling in coastal waters: Illustration over the eastern continental shelf of the Bay of Biscay. Remote Sensing of Environment 95, 29 – 46.

Gowen, R.J., Mills, D.K., Trimmer, M., Nedwell, D.B., 2000. Production and its fate in two coastal regions of the Irish Sea: the influence of anthropogenic nutrients. Marine Ecology Progress Series 208, 51 – 64.

Hu, C., Carder, K.L., Muller-Karger, F.E., 2000. Atmospheric correction of SeaWiFS imagery over turbid coastal waters: a practical method. Remote Sensing of Environment 74, 195 – 206.

Jeffrey, S.W., Humphrey, G.F., 1975. New spectrophotometric equations for determining chlorophylls *a*, *b*, c_1 and c_2 in higher plants, algae and natural phytoplankton. Biochemie und Physiologie der Pflanzen 167, 191 – 194.

Joint, J., Groom, S.B., 2000. Estimation of phytoplankton production from space: current status and future potential of satellite remote sensing. Journal of Experimental Marine Biology and Ecology 250, 233 – 255.

Land, P.E., Haigh, J. D., 1997. Atmospheric correction over Case 2 waters with an iterative fitting algorithm: relative humidity effects. Applied Optics 36, 9448 – 9455.

Lavender, S.J., Pinkerton, M.H., Moore, G.F., Aiken, J., Blondeau-Patissier, D., 2005. Modification to the atmospheric correction of SeaWiFS ocean colour images over turbid waters. Continental Shelf Research 25, 539 – 555.

Maritorena, S., Siegel, D.A., Peterson, A.R., 2002. Optimization of a semianalytical ocean color model for global-scale applications. Applied Optics 41, 2705 – 2714.

McKee, D., Cunningham, A., 2005 Evidence for wavelength dependence of the particle scattering phase function and its implication for modelling radiance transfer in shelf seas. Applied Optics 44, 126-135.

McKee, D., Cunningham, A., 2006. Identification and characterisation of two optical water types in the Irish Sea from *in situ* inherent optical properties and seawater constituents. Estuarine, Coastal and Shelf Science 68, 305-316.

Moore, G.F., Aiken, J., Lavender, S.J., 1999. The atmospheric correction of water colour and the quantitative retrieval of suspended particulate matter in Case II waters: application to MERIS. International Journal of Remote Sensing 20(9), 1713 - 1733.

Morel, A., Prieur, L., 1977. Analysis of variations in ocean colour. Limnology and Oceanography 22, 709 – 722.

Mueller, J.L., Austin, R.W., 1995. Ocean optics protocols for SeaWiFS Validation, Revision 1. NASA Tech. Memo. 104566: SeaWiFS Technical Report Series Volume 25, S.B. Hooker, E.R. Firestone and J.G. Acker, Eds, NASA Goddard Space Flight Center, Greenbelt, Maryland, pp1-2.

Mueller, J.L., 2000. SeaWiFS algorithm for the diffuse attenuation coefficient, K(490), using water-leaving radiances at 490 and 555nm. NASA Tech. Memo. 2000-206892: SeaWiFS Postlaunch Technical Report Series Volume 11, S.B. Hooker and E.R. Firestone, Eds, NASA Goddard Space Flight Center, Greenbelt, Maryland, pp24-27.

O'Reilly, J.E., Maritorena, S., Siegel, D.A., O'Brien, M.C., Toole, D., Mitchell, B.G., Kahru, M., Chavez, F.P., Strutton, P., Cota, G.F., Hooker, S.B., McClain, C.R., Carder, K.L., Müller-Karger, F., Harding, L., Magnuson, A., Phinney, D., Moore, G.F., Aiken, J., Arrigo, K.R., Letelier, R., Culver, M., 2000. Ocean Color Chlorophyll *a* Algorithms for SeaWiFS, OC2, and OC4: Version 4. NASA Tech. Memo. 2000-206892: SeaWiFS Postlaunch Technical Report Series Volume 11, S.B. Hooker and E.R. Firestone, Eds, NASA Goddard Space Flight Center, Greenbelt, Maryland, pp9-23.

Pegau, W.S., Gray, D., Zaneveld, J.R.V., 1997. Absorption and attenuation of visible and near-infrared light in water: dependence on temperature and salinity. Applied Optics 36, 6035 – 6046.

Raine, R., O'Boyle, S., O'Higgins, J., White, M., Patching, J., Cahill, B., McMahon, T., 2001. A satellite and field portrait of a *Karenia mikimotoi* bloom off the south west coast of Ireland, August 1998. Hydrobiologia 465, 187 – 193.

Sathyendranath, S., 2000. Remote sensing of ocean colour in coastal, and other optically complex waters. International Colour Coordinating Group Report No. 3, 145 pp.

Smith, R.C., Baker, K., 1981. Optical properties of the clearest natural waters (200-800 nm). Applied Optics, 20, 177 – 184.

Smith, C.N., Stewart, T.H., MacDonald, P., 2003. Results from an intensive measurement programme for suspended particulate matter in a region of the Irish Sea between Anglesey and the Isles of Man. Continental Shelf Research 23, 1005 – 1018.

Smyth, T. J., Moore G.F., Groom, S.B., Land, P.E., Tyrell, T., 2002. Optical modelling and measurements of a coccolithophore bloom. Applied Optics 41, 7679 – 7688.

Toole, D.A., Siegel, D.A., 2001. Modes and mechanisms of ocean colour variability in the Santa Barbara Channel. Journal of Geophysical Research-Oceans, 106(C11), 26985-27000.

Wang, J., Cota, G.F., 2003. Remote-sensing reflectance in the Beaufort and Chukchi seas: observations and models. Applied Optics 42, 2754-2765.

Zaneveld, J.R.V., Kitchen, J.C. and Moore, C., 1994. The scattering error correction of reflecting-tube absorption meters. Proc. Ocean Optics XII. Jaffe, J.S. (Ed.), SPIE Vol. 2258: 44-55.

Figures

Figure 1 Map showing the location of 102 stations in the Irish and Celtic Seas (×) together with 19 additional stations in the Bristol Channel (+).

Figure 2 Values of the diffuse attenuation coefficient for downward irradiance at 490 nm, $K_d(490)$, calculated using the standard *SeaDAS* algorithm plotted against those measured *in situ* using a profiling radiometer.

Figure 3 Values of the concentration of chlorophyll *a* (*Chl*: mg m^{-3}) calculated using the standard *SeaDAS OC4v4* algorithm plotted against direct determinations from filtered samples. Dashed lines indicate the ±35% SeaWiFS mission target for *Chl* retrieval.

Figure 4 Particulate backscattering (b_{bp}) plotted against non-water absorption (a_n) at 676 nm showing the existence of two data clusters, Groups A and B. These were separated by a straight line with an empirical slope of 0.5.

Figure 5 Normalised water leaving radiance spectra for twelve stations, six each for water types A and B. Group A nL_w spectra are generally higher than Group B spectra at green and red wavelengths, but they overlap to a greater extent in the blue.

Figure 6 Values of $K_d(490)$ measured *in situ* plotted against the ratio of normalised water leaving radiances (nL_w) derived from in situ radiometry in the SeaWiFS 490 and 555 nm wavebands. The solid line was generated using the standard *SeaDAS*

parameters and approximately fits Group B data. The broken line was generated using adjusted parameter values and provides a much better fit to the Group A data.

Figure 7 Concentration of chlorophyll *a* determined from filtered water samples plotted against *R*, the logarithm of the maximum value of the in situ blue/green reflectance ratio used in *OC4v4*. The dotted line was generated using the *OC4v4* algorithm with standard parameter values. The broken and solid lines represent best fits of the same function with adjusted parameters to the Group A and B data respectively. Note that the standard algorithm overestimates *Chl* for both groups of data.

Figure 8 Improved recovery of $K_d(490)$ values resulting from the use of the dual algorithm (Equation 5) on the main data set from the Irish / Celtic Sea. The dual algorithm approach, in which parameter values are tuned to water type, clearly describes the data set better than the standard single algorithm (Figure 2). The best–fit regression line (dashed) and the 1:1 line (solid) are also shown.

Figure 9 Chlorophyll concentrations recovered from the main Irish / Celtic Sea data set using the dual algorithm (Equation 6) largely fall within the ±35% error boundaries specified for the SeaWiFS chlorophyll product. The dual algorithm approach, based on identification of optical water type, successfully describes the data set better than the standard *OC4v4* algorithm (Figure 3).

Figure 10 Values of $K_d(490)$ calculated using either the standard *SeaDAS* algorithm (closed symbols) or the new dual algorithm (Equation 5 – open symbols) plotted

against measured values of $K_d(490)$ for the Bristol Channel data set. Best-fit regressions are shown as dashed lines together with the 1:1 line (solid). The dual algorithm clearly provides improved estimates of $K_d(490)$ for turbid waters.

Figure 11 Values of *Chl* calculated using either the standard *SeaDAS OC4v4* algorithm (closed symbols) or the dual algorithm (Equation 6 – open symbols) plotted against direct determinations of *Chl* for the Bristol Channel data set. The dual algorithm eliminates the systematic overestimate of *Chl* by *OC4v4* in turbid waters.

Figure 1. Optical water type discrimination and tuning remote sensing band-ratio algorithms: Application to retrieval of chlorophyll and Kd(490) in the Irish and Celtic Seas

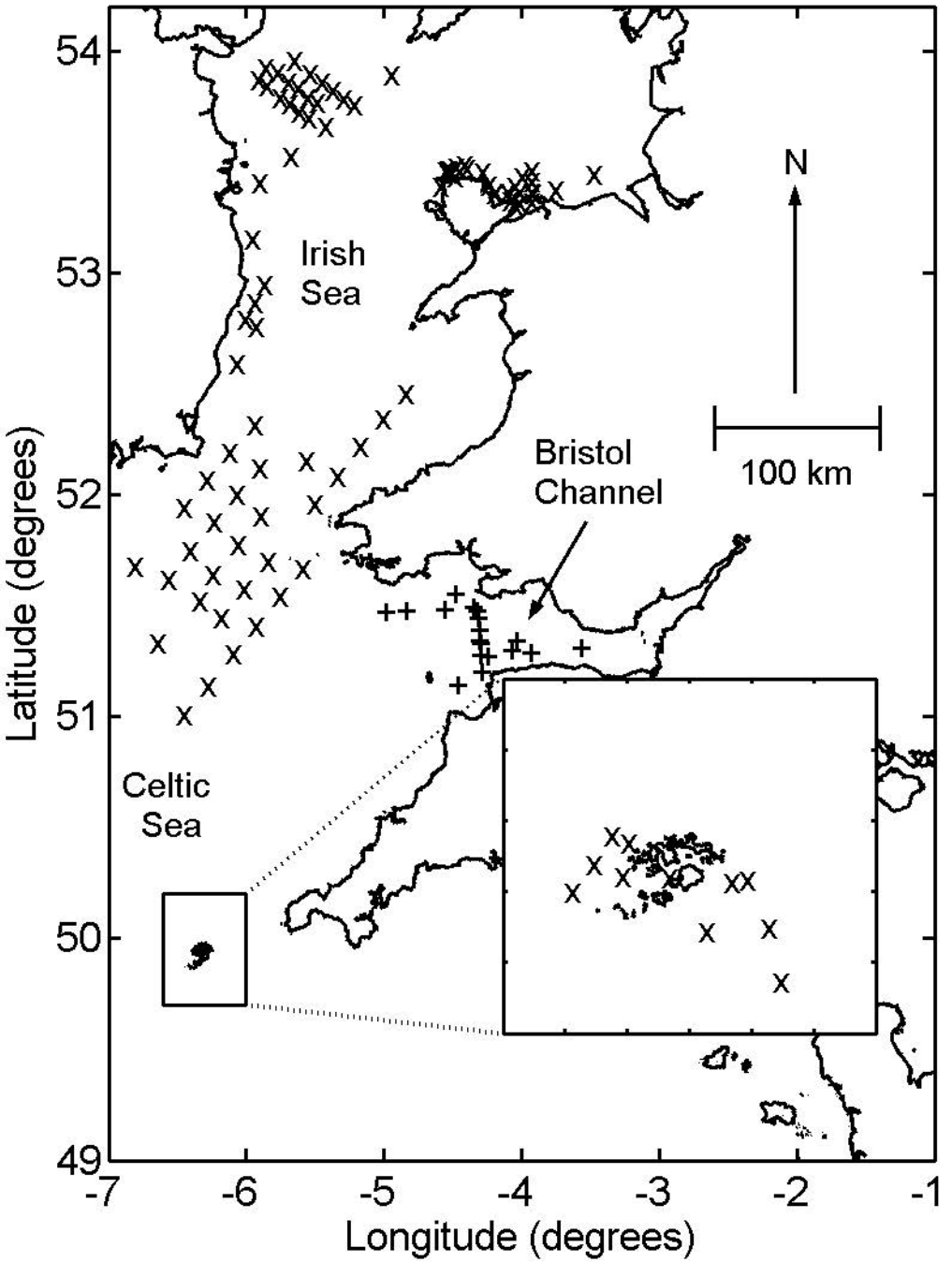

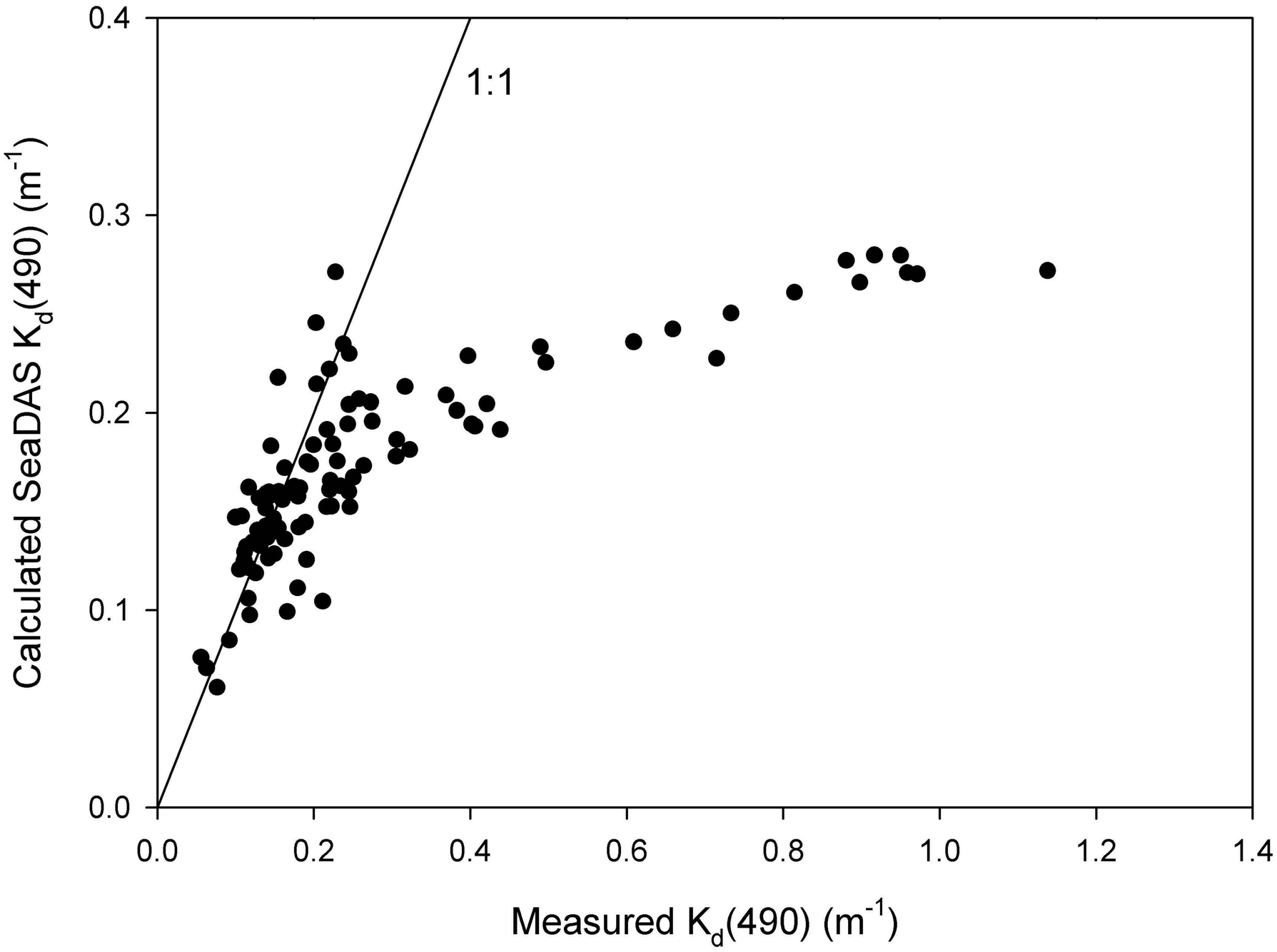

Figure 2 - McKee et al

Optical water type discrimination and tuning remote sensing band-ratio algorithms:
Application to retrieval of chlorophyll and Kd(490) in the Irish and Celtic Seas

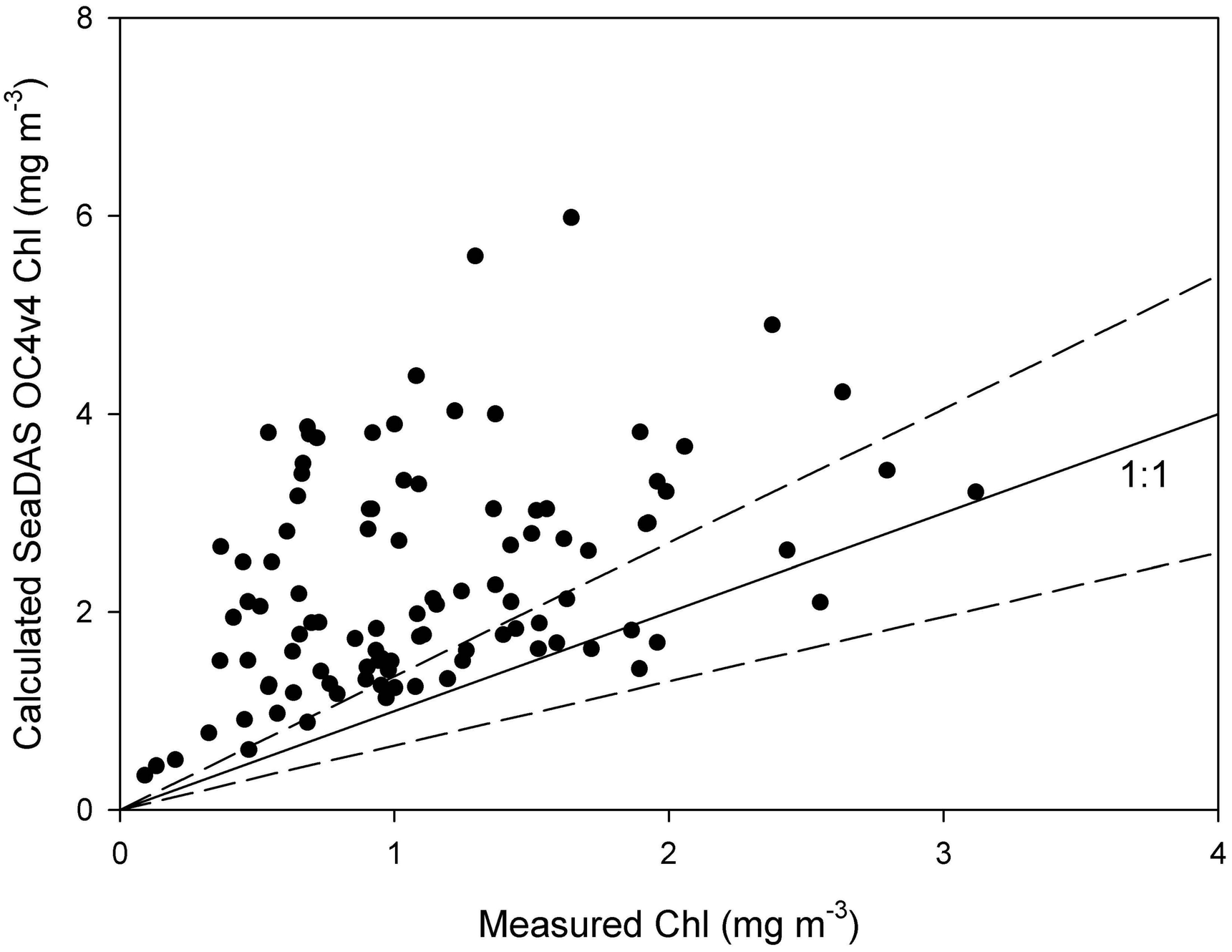

Figure 3 - McKee et al

Optical water type discrimination and tuning remote sensing band-ratio algorithms:
Application to retrieval of chlorophyll and Kd(490) in the Irish and Celtic Seas

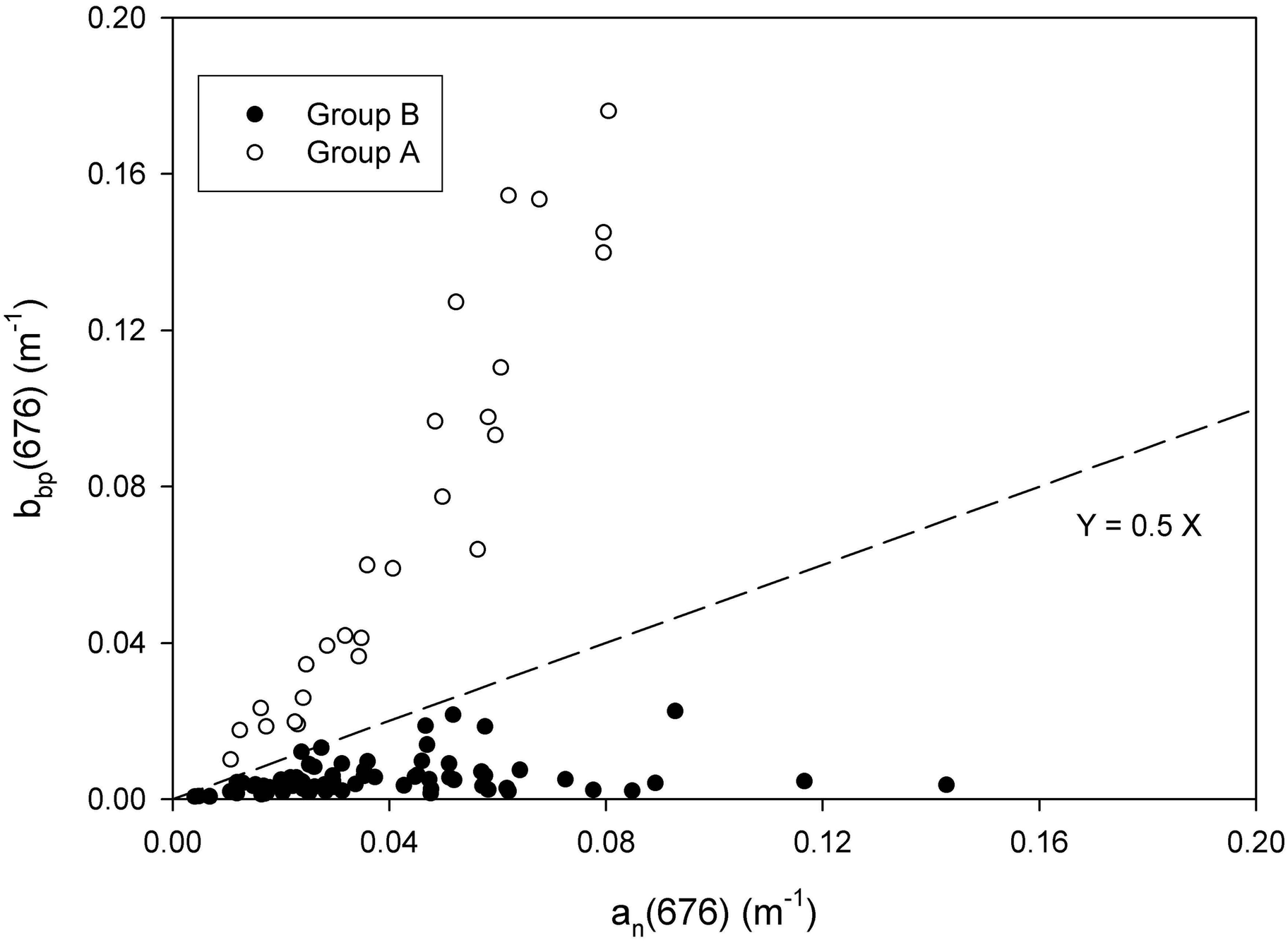

Figure 4 - McKee et al

Optical water type discrimination and tuning remote sensing band-ratio algorithms:
Application to retrieval of chlorophyll and Kd(490) in the Irish and Celtic Seas

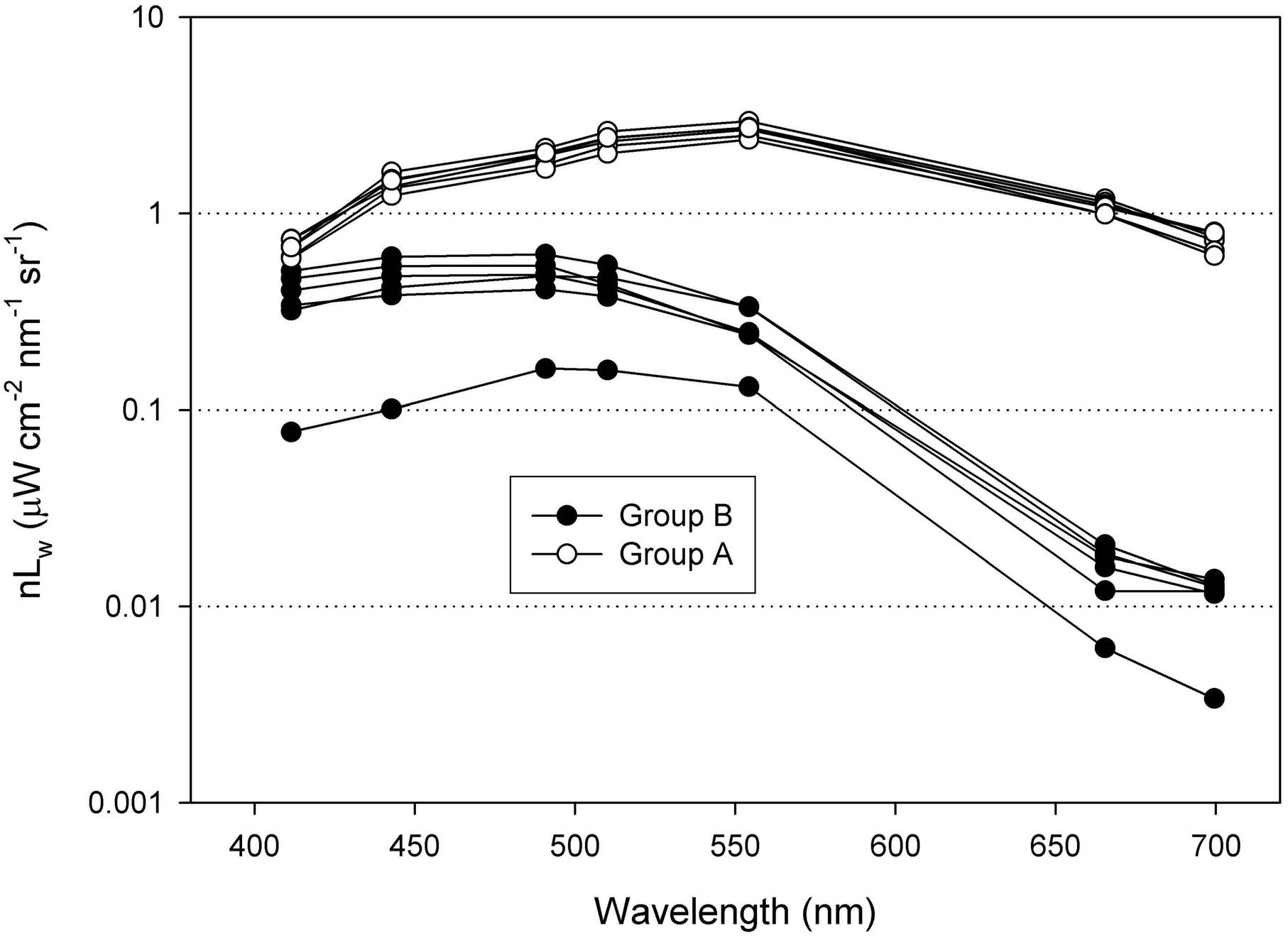

Figure 5 - McKee et al

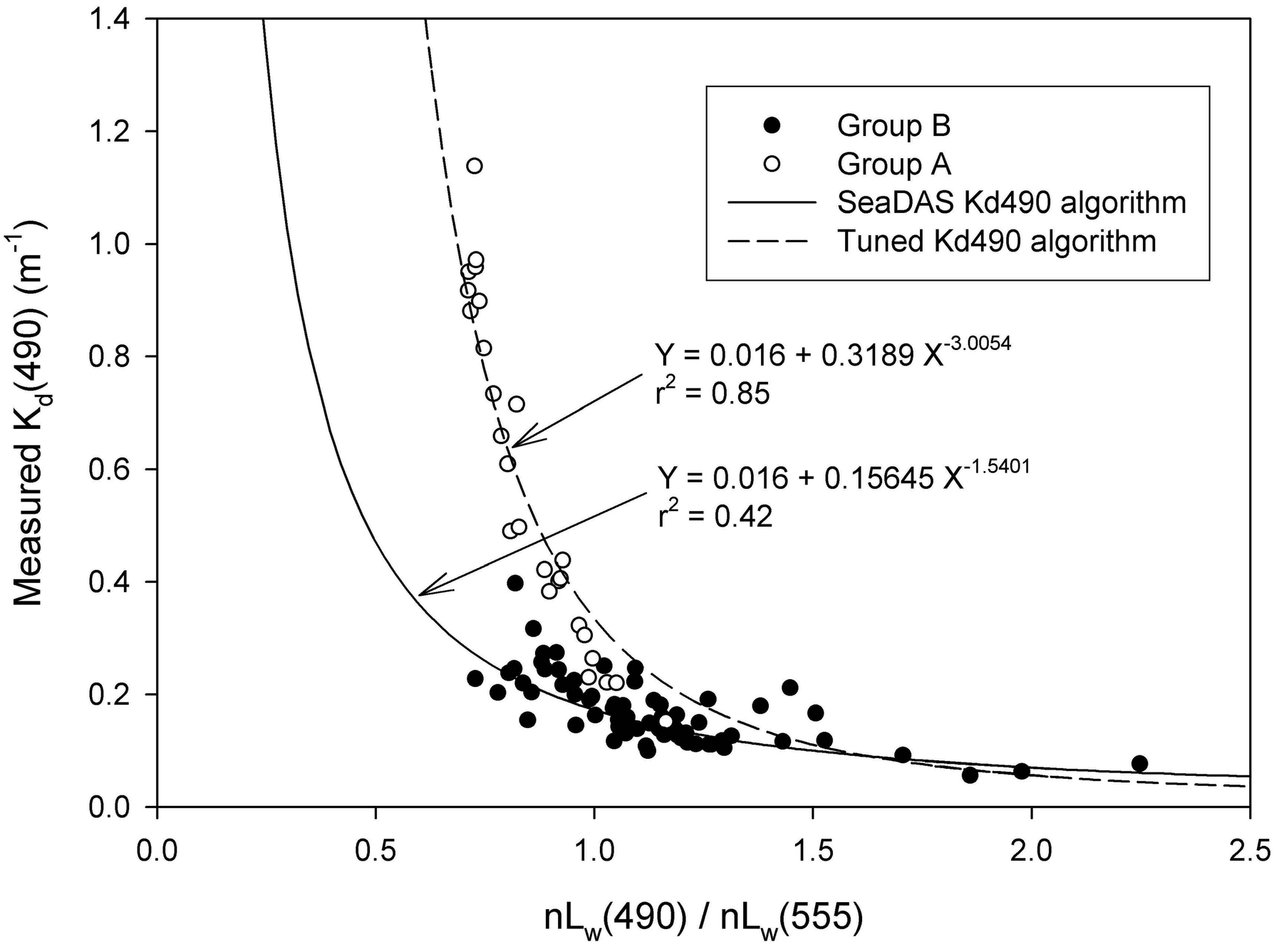

Figure 6 - McKee et al

Optical water type discrimination and tuning remote sensing band-ratio algorithms:
Application to retrieval of chlorophyll and Kd(490) in the Irish and Celtic Seas

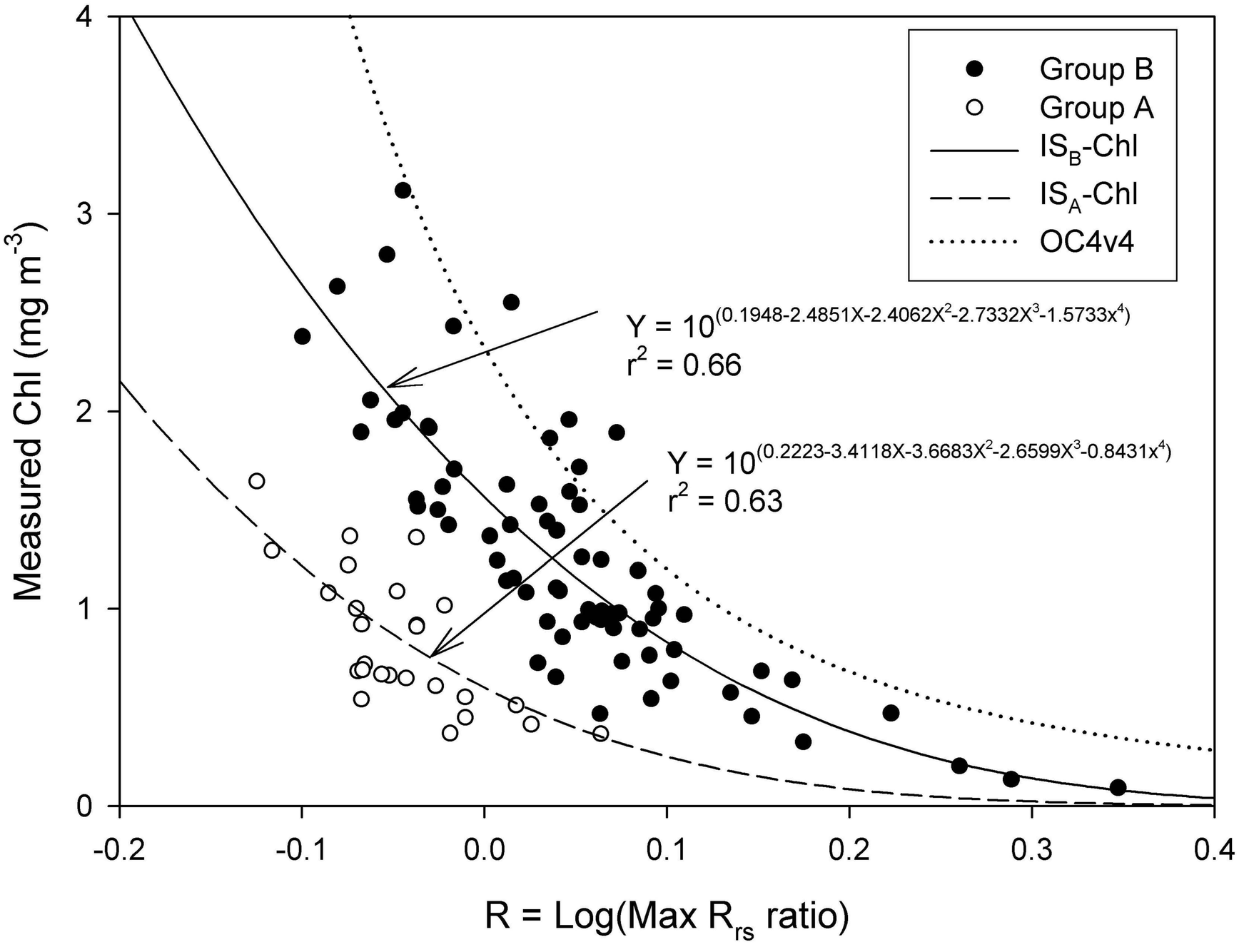

Figure 7 - McKee et al

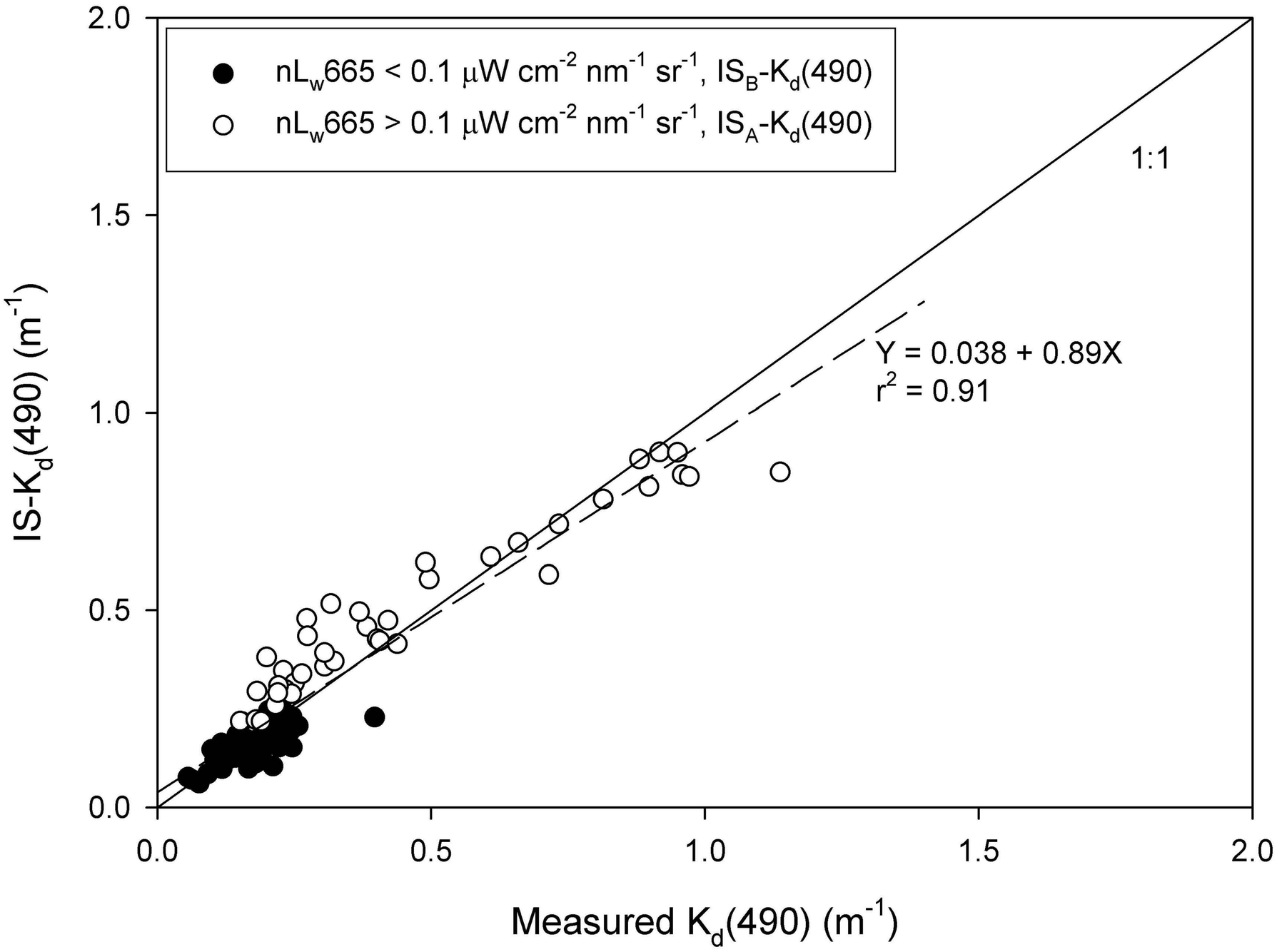

Figure 8 - McKee et al

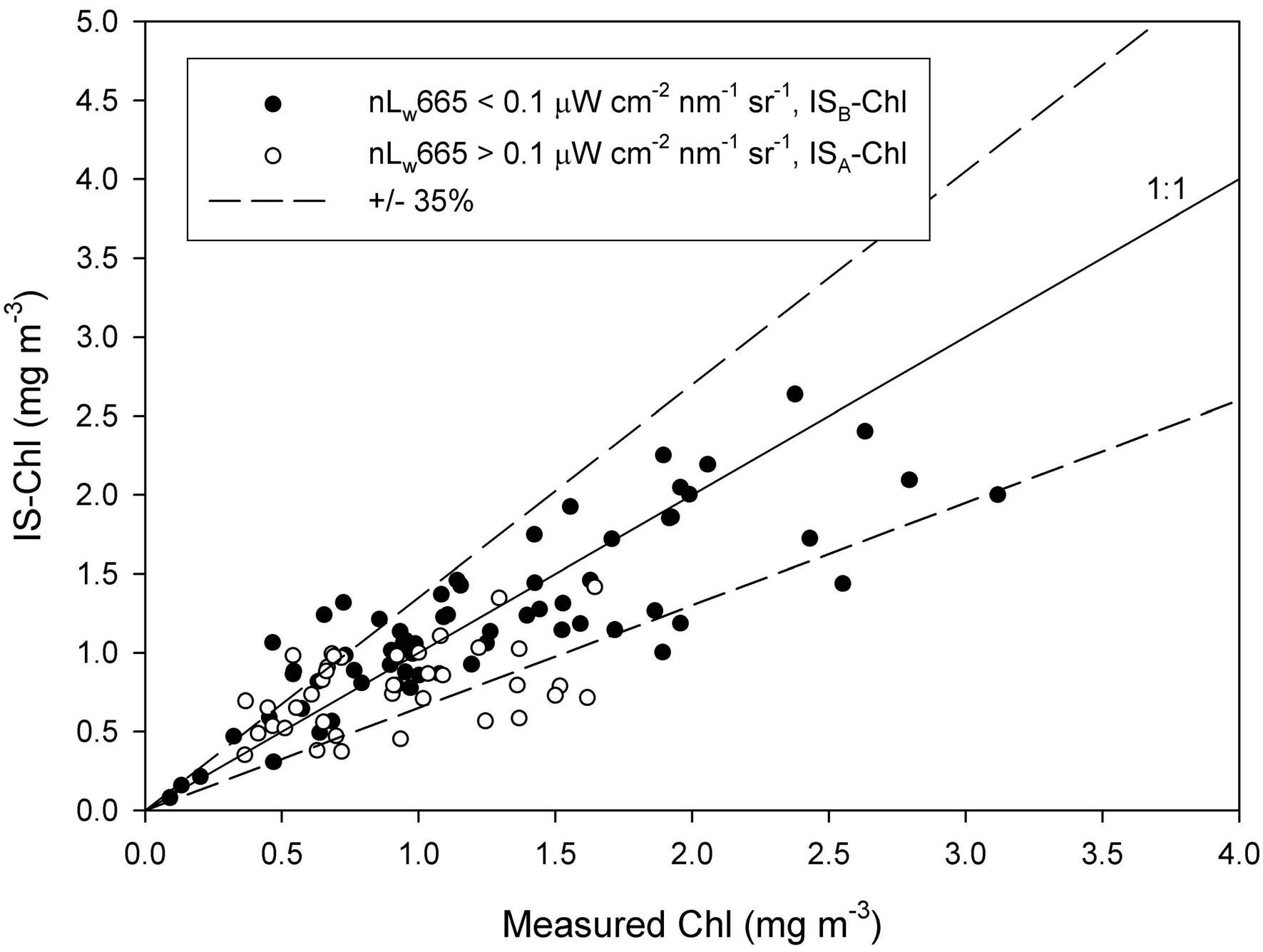

Figure 9 - McKee et al

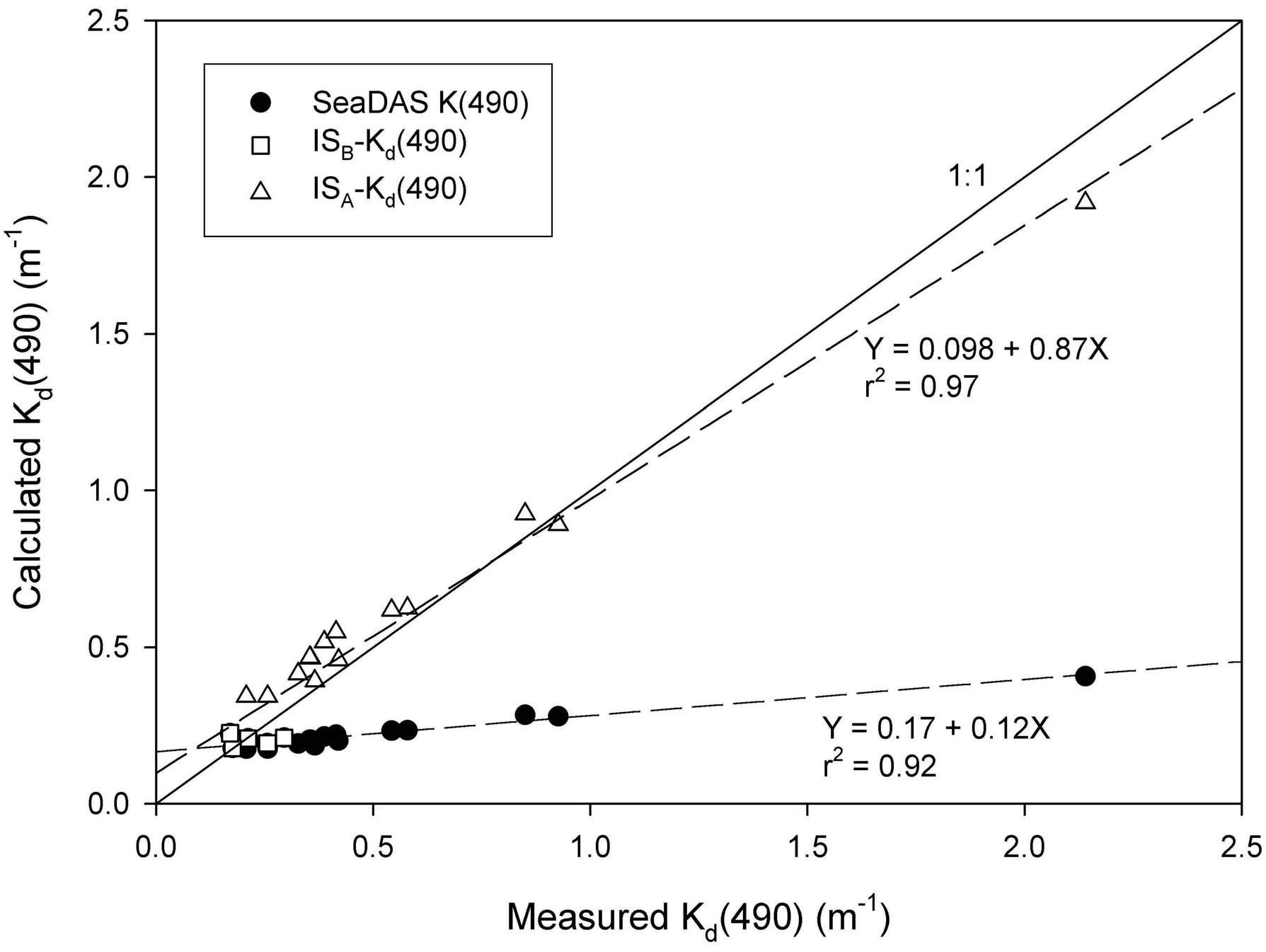

Figure 10 - McKee et al

Optical water type discrimination and tuning remote sensing band-ratio algorithms:
Application to retrieval of chlorophyll and Kd(490) in the Irish and Celtic Seas

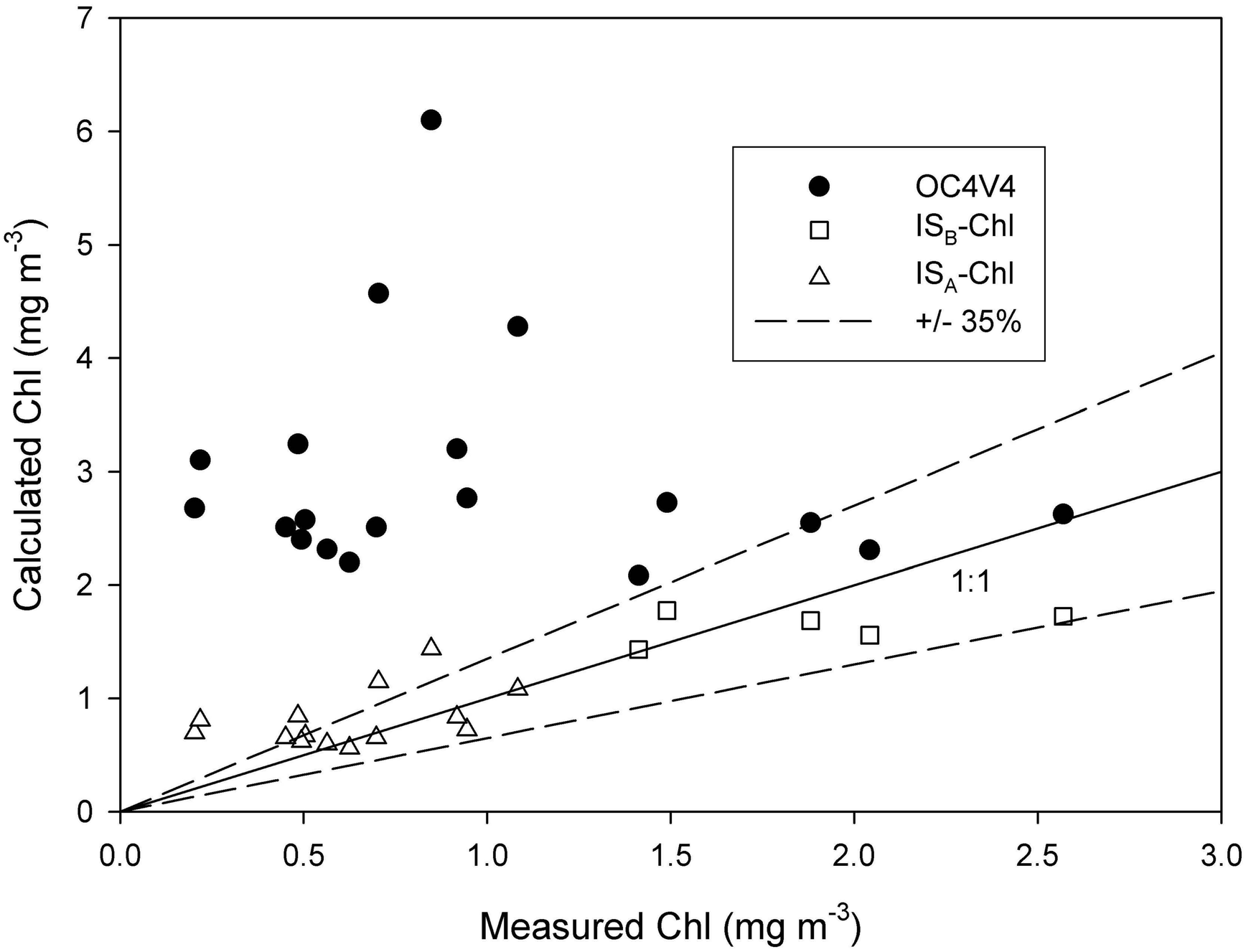

Figure 11 - McKee et al